Int. J. Solids Structures Vol. 29, No. 24, pp. 3065–3085, 1992
Printed in Great Britain.

0020-7683/92 $5.00 + .00

PERIODIC LOADING IN FRICTIONAL CONTACT FORMULATED BY COMPLEMENTARITY

SE BIN IM and BYUNG MAN KWAK
Department of Mechanical Engineering, Korea Advanced Institute of Science and Technology, 373-1, Kuseong-Dong, Yuseong-Gu, Taejon, 305-701, Korea

(*Received* 8 *February* 1992; *in revised form* 25 *May* 1992)

Abstract—In the case of frictional contact problems subjected to periodic loading, due to non-uniqueness and non-linearity, the size of a load increment must be suitably determined to obtain the proper, physically meaningful path of response history. A method of an automatic load increment is proposed based on the sensitivity analysis of the solution with respect to the load scale parameter. Frictional contact conditions are formulated by complementarity and sensitivity analysis of the solutions with respect to the applied load, using the parametric optimal design theory. As illustrative examples, a layer pressed against a half-plane by a uniform pressure and subjected to a tangential force varying periodically in time is tested and compared with the solutions by Comninou and Barber (1983, *Int. J. Solids Structures* **19**, 533–539). As a practical problem, a valve-cotter system of a small engine subjected to a periodic loading is solved as a three body contact problem.

1. INTRODUCTION

In the literature, solution methods of a frictional contact problem can be divided into two categories. In the first category, the solution is sought iteratively by a trial and error method until it satisfies contact and friction conditions (Hanson and Keer, 1989; Rahman *et al.*, 1984). Second, the contact problem is reformulated as mathematical problems such as a variational inequality or a complementarity problem. The variational inequality formulation is useful in obtaining mathematical properties of the solution such as existence and uniqueness (Duvaut and Lions, 1976; Panagiotopoulos, 1985), however it has been limited to the case in which either normal pressure or contact are known, or some mathematical assumptions on smoothness of friction law are used (Oden and Pires, 1983a, b). On the other hand, Klarbring (1986) presented a complementarity problem formulation where Coulomb friction law is treated as a subdifferential law under the restriction that contact status is constant during an incremental loading step. All these methods are lacking a unified complete theoretical basis. They are heuristic or have rather serious limiting assumptions. Recently, (Kwak and Lee, 1988; Kwak, 1990, 1991) a complementarity principle has been derived directly, which is mathematically complete in describing the frictional problem. For the two-dimensional case, this leads to a linear complementarity problem (LCP). In the general three-dimensional case, by introducing a polyhedral law of friction, the problem can be transformed to a linear complementarity problem.

Because of non-linearity of contact problem, an incremental analysis is inevitable. Since the physical state is unique for a given path of loading, the problem is how to guarantee the correct path numerically. This will restrict the amount of an incremental loading step. One common method is that the applied load is incremented by an amount which causes a change in the contact status (Okamoto and Nakazawa, 1979; Torstenfelt, 1984).

In this paper, a sensitivity analysis with respect to the loading scale parameter is systematically used to obtain the size of an incremental step. It is based on the formulation by complementarity (Kwak and Lee, 1988; Kwak, 1991), and the parametric optimal design theory (Kwak and Haug, 1976) is utilized to derive the sensitivity formula. The sensitivity of a solution with respect to the perturbations of problem parameters has been studied in the literature, but with different purposes. In general mathematical programming problems, it is developed by differentiation of the Kuhn–Tucker conditions (Fiacco and Ghaemi, 1982; Jittorntrum, 1984; Tobin, 1986). In the case of a variational inequality formulation,

it is obtained as the solution of an auxiliary variational inequality and is a directional derivative (Bendsoe *et al.*, 1985). Using this, Sokolowski (1988) derived a sensitivity formula with respect to problem parameters for a contact problem with given friction. Haslinger and Neittaanmaki (1988) also derived the sensitivity formula of contact problem with given friction by variational inequality and illustrated it by simple examples. For completeness a general kinematic description with an updated Lagrangian formulation is adopted and finite element method used for discretization. Large deformation problems in this setting have been treated earlier (Joo and Kwak, 1986) but no friction is included.

To show the validity and usability of the proposed method, a layer pressed against a half-plane by a uniform pressure and subjected to a tangential force varying periodically in time is simulated and compared with the solutions by Comninou and Barber (1983). As a more practical application, a valve-cotter system of a motorcycle engine subjected to a periodic loading is solved as an axisymmetric three body contact problem.

2. COMPLEMENTARITY PROBLEM FORMULATION FOR TWO-DIMENSIONAL CONTACT PROBLEM WITH COULOMB FRICTION

The updated Lagrangian formulation referring to current state t is employed for loading-path dependent nature of friction phenomena. Large displacement and material non-linearity are also considered. The formulation of the internal equilibrium is first summarized and the finite element method is introduced for discretization.

The principle of virtual work at $t+\Delta t$ is expressed as

$$\int_{t+\Delta t_V} {}^{t+\Delta t}\tau_{ij}\,\delta\,{}^{t+\Delta t}e_{ij}\,\mathrm{d}V = {}^{t+\Delta t}\delta R, \tag{1}$$

where ${}^{t+\Delta t}\delta R$ is the external virtual work, and ${}^{t+\Delta t}\tau_{ij}$ and ${}^{t+\Delta t}e_{ij}$ are the Cartesian components of the Cauchy stress tensor and the Cartesian components of the infinitesimal strain tensor, respectively.

Since the configuration of the body at time $t+\Delta t$ is not known, the equilibrium equation of the body is established in the current configuration t. Employing the 2nd Piola–Kirchhoff stress and the Green–Lagrangian strain which are energetically conjugate each other, the principle of virtual work at time $t+\Delta t$ is then rewritten (Bathe, 1982):

$$\int_{t_V} {}_t^{t+\Delta t}S_{ij}\,\delta\,{}_t^{t+\Delta t}\varepsilon_{ij}\,\mathrm{d}V = {}^{t+\Delta t}\delta R. \tag{2}$$

The Green–Lagrangian strain tensor has the following expression:

$$\varepsilon_{ij} = \tfrac{1}{2}(u_{i,j}+u_{j,i}) + \tfrac{1}{2}u_{k,i}u_{k,j}. \tag{3}$$

The 2nd Piola–Kirchhoff stress and the Green–Lagrangian strain are decomposed as

$${}_t^{t+\Delta t}S_{ij} = {}^t\tau_{ij} + {}_tS_{ij}, \tag{4}$$

$${}_t^{t+\Delta t}\varepsilon_{ij} = {}_te_{ij} + {}_t\eta_{ij}, \tag{5}$$

where

$${}_te_{ij} = \tfrac{1}{2}({}_tu_{i,j} + {}_tu_{j,i}) \quad \text{and} \quad {}_t\eta_{ij} = \tfrac{1}{2}{}_tu_{k,i}\,{}_tu_{k,j}. \tag{6}$$

The stress and strain relationship for an incremental loading step is given by

$${}_tS_{ij} = {}_tC_{ijkl}\,{}_t\varepsilon_{kl}, \tag{7}$$

where ${}_tC_{ijkl}$ is the constitutive coefficient at current time t.

When eqns (4), (5) and (7) are substituted, eqn (2) becomes

$$\int_{t_V} {}_tC_{ijkl}\,{}_te_{kl}\delta_t\varepsilon_{ij}\,\mathrm{d}V+\int_{t_V} {}^t\tau_{ij}\delta_t\eta_{ij}\,\mathrm{d}V={}^{t+\Delta t}\delta R-\int_{t_V} {}^t\tau_{ij}\delta_t e_{ij}\,\mathrm{d}V. \tag{8}$$

Discarding higher order terms in eqn (8), the following equation is obtained:

$$\int_{t_V} {}_tC_{ijkl}\,{}_te_{kl}\delta_t e_{ij}\,\mathrm{d}V+\int_{t_V} {}^t\tau_{ij}\delta_t\eta_{ij}\,\mathrm{d}V={}^{t+\Delta t}\delta R-\int_{t_V} {}^t\tau_{ij}\delta_t e_{ij}\,\mathrm{d}V. \tag{9}$$

Employing suitable shape functions, displacement increments u_i are expressed as

$$u_i(x_1, x_2, x_3)=\sum_k \phi_{ik}(x_1, x_2, x_3)\hat{u}_k, \tag{10}$$

where $\phi_{ik}(x_1, x_2, x_3)$ and $\hat{u}_k$ represent shape functions and nodal displacement increments, respectively. Following the usual finite element discretization procedure, a matrix equation corresponding to eqn (9) is obtained:

$$(\mathbf{K}_L+\mathbf{K}_{NL})\mathbf{u}={}^{t+\Delta t}\mathbf{R}-{}^{t+\Delta t}\mathbf{F}, \tag{11}$$

where $\mathbf{u}$ is the nodal displacement increment vector and,

$$K_L(i,j)=\int_{t_V} C_{klpq}\frac{\partial\phi_{ki}}{\partial x_l}\frac{\partial\phi_{pj}}{\partial x_q}\,\mathrm{d}V, \tag{12}$$

$$K_{NL}(i,j)=\int_{t_V} {}^t\tau_{kl}\frac{\partial\phi_{pi}}{\partial x_k}\frac{\partial\phi_{pj}}{\partial x_l}\,\mathrm{d}V, \tag{13}$$

$${}^{t+\Delta t}F(i)=\int_{t_V} {}^t\tau_{kl}\frac{\partial\phi_{ki}}{\partial x_l}\,\mathrm{d}V, \tag{14}$$

$${}^{t+\Delta t}R(i)=\int_{t+\Delta t_V} {}^{t+\Delta t}f_k^B\phi_{ki}\,\mathrm{d}V+\int_{t+\Delta t_{\Gamma_f}} {}^{t+\Delta t}f_k^S\phi_{ki}\,\mathrm{d}\Gamma+\int_{t+\Delta t_{\Gamma_c}} {}^{t+\Delta t}f_k^C\phi_{ki}\,\mathrm{d}\Gamma, \tag{15}$$

where f_k^B is body force vector, f_k^S surface traction vector and f_k^C unknown contact traction vector at the potential contact surface which is selected sufficiently large to cover the real contact area.

Decomposing $\mathbf{u}$ into the nodal displacement increments on the potential contact surface, $\mathbf{u}_c$, and the internal nodal displacement increments, $\mathbf{u}_i$, the matrix equation (11) can be rewritten in a partitioned form as

$$\begin{bmatrix}\mathbf{K}_{ii} & \mathbf{K}_{ic}\\ \mathbf{K}_{ci} & \mathbf{K}_{cc}\end{bmatrix}\begin{Bmatrix}\mathbf{u}_i\\ \mathbf{u}_c\end{Bmatrix}=\begin{Bmatrix}\mathbf{F}_i\\ \mathbf{F}_c\end{Bmatrix}, \tag{16}$$

where $\mathbf{F}_i$ and $\mathbf{F}_c$ are corresponding force vectors. After statically condensing out the internal degrees of freedom $\mathbf{u}_i$, the matrix equation for $\mathbf{u}_c$ is obtained:

$$\hat{\mathbf{K}}\mathbf{u}_c=\mathbf{F}_c-\mathbf{K}_f\mathbf{F}_i, \tag{17}$$

where

$$\hat{\mathbf{K}}=\mathbf{K}_{cc}-\mathbf{K}_{ci}\mathbf{K}_{ii}^{-1}\mathbf{K}_{ic},$$

$$\mathbf{K}_f=\mathbf{K}_{ci}\mathbf{K}_{ii}^{-1}.$$

So the relationship between the displacement increment and the force at the potential contact surface for the kth body is expressed as

$$\mathbf{u}_c^k = \mathbf{B}^k \mathbf{F}_c^k + \mathbf{T}^k \mathbf{F}_r^k, \tag{18}$$

where $\mathbf{B}^k = \hat{\mathbf{K}}^{-1}$ and $\mathbf{T}^k = -\hat{\mathbf{K}}^{-1}\mathbf{K}_f$.

The displacement increment $\mathbf{u}_c^k$ and force $\mathbf{F}_c^k$ in eqn (18) are unknown and these must satisfy contact and friction conditions described below (Kwak and Lee, 1988; Kwak, 1991). The formulation is briefly described using a two-dimensional case. It is noted that the three-dimensional case is somewhat different from the two-dimensional case, and the reader is referred to Kwak (1991).

(1) *Global equilibrium*

The formulation is described for a two-body contact without loss of generality. Body 2 is assumed restrained against any rigid body displacements, while body 1 is allowed for rigid body displacement denoted by q_i as shown in Fig. 1. For body 1, where rigid body motions are allowed, all the external forces and the contact forces should be in equilibrium. For configuration at $t+\Delta t$, from the principle of virtual displacements, the global equilibrium equation for body 1 is obtained as follows:

$$\int_{t+\Delta t\Gamma_f^1} {}^{t+\Delta t}F_i H_{ij}^{t+\Delta t}\,\mathrm{d}\Gamma + \int_{t+\Delta t\Gamma_c^1} {}^{t+\Delta t}S_i A_{ij}^{t+\Delta t}\,\mathrm{d}\Gamma = 0, \tag{19}$$

where the coefficient matrices A_{ij} and H_{ij} represent the rigid body displacements of points of ${}^{t+\Delta t}\Gamma_c$ and ${}^{t+\Delta t}\Gamma_f$ in the ith coordinate direction due to a unit displacement in the jth rigid body degree of freedom q_j, respectively. And F_i and S_i denote traction vectors corresponding to the external and contact forces, respectively.

(2) *Impenetration condition*

Let the opposing surfaces in the potential contact region at configuration t be described as shown in Fig. 2:

$$g^1(a_i^1) = 0 \quad \text{and} \quad g^2(a_i^2) = 0. \tag{20}$$

Then the impenetration condition is expressed as; for any point a_i^1

$$g^1(a_i^2 + u_i^2(a_i^2) - \hat{u}_i^1(a_i^1)) \geqslant 0, \tag{21}$$

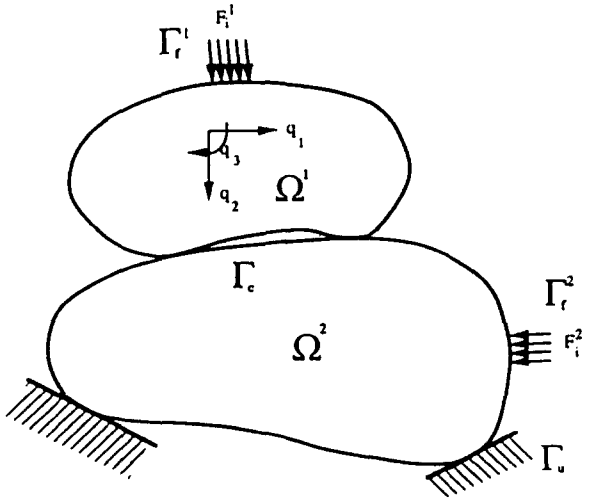

Fig. 1. Two bodies in contact (Kwak, 1991).

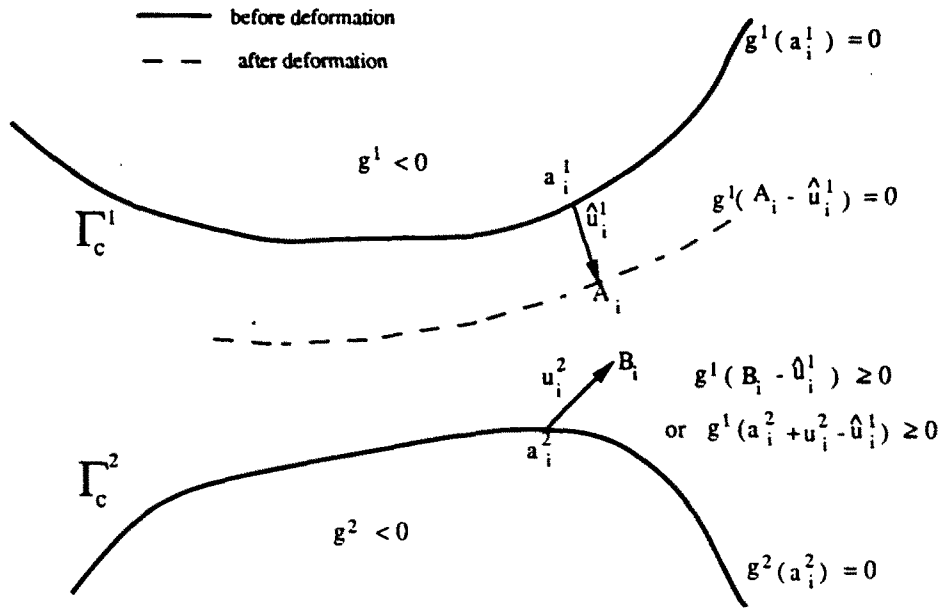

Fig. 2. General description of impenetration condition (Kwak, 1991).

for all a_t^2 satisfying $g^2(a_t^2)=0$ on Γ_c^2, where

$$\hat{u}_t^1(a_t^1)=u_t^1(a_t^1)+\alpha_{tj}q_j. \tag{22}$$

The coefficient α_{tj} represents the displacement of a_t^1 due to the rigid body displacement q_j. It is noted that $g^1(a_t^2+u_t^2(a_t^2)-\hat{u}_t^1(a_t^1))$ essentially denotes the gap between the points a_t^1 and a_t^2 after deformation during Δt. Let

$$D_n(a_t^1)=\min_{a_t^2} g^1(a_t^2+u_t^2(a_t^2)-\hat{u}_t^1(a_t^1)) \tag{23}$$

such that the value $D_n(a_t^1)$ denotes the distance from the particle a_t^1 to the surface $g^2(a_t^2)=0$ after deformation. The point a_t^1 and the minimizing point a_t^2 are called the contacting pair. Then the impenetration condition can be simply expressed as

$$D_n(a_t^1)\geq 0 \quad \text{for all } a_t^1 \text{ such that } g^1(a_t^1)=0. \tag{24}$$

By considering only the first order terms of Taylor's expansion, eqn (23) can be rewritten for a mating contact pair as follows:

$$D_n(a_t^1)=\beta+\mathbf{n}^1(\mathbf{u}^2(a_t^2)-\mathbf{u}^1(a_t^1)-\mathbf{A}\mathbf{q}), \tag{25}$$

where

$$\beta=g^1(a_t^2), \quad n_k=\left.\frac{\partial g^1}{\partial x_k}\right|_{a_t^1,a_t^2}.$$

Since either contact gap $D_n(a_t^1)$ or contact normal force ${}^{t+\Delta t}P$ between two mating contact pairs after load increment Δt must be equal to zero, the following condition is also satisfied:

$${}^{t+\Delta t}P\cdot D_n(a_t^1)=0 \quad \text{for all } a_t^1 \text{ on } \Gamma_c^1. \tag{26}$$

(3) *Coulomb friction condition*

From the Coulomb friction law, the contact tangential force ${}^{t+\Delta t}S_T$ must satisfy the following relation:

$$-\mu^{t+\Delta t}P \leqslant {}^{t+\Delta t}S_T \leqslant \mu^{t+\Delta t}P, \tag{27}$$

where μ is a friction coefficient. If $|{}^{t+\Delta t}S_T| < \mu^{t+\Delta t}P$, then there is no relative tangential displacement. And, if $|{}^{t+\Delta t}S_T| = {}^{t+\Delta t}P$, slip is imminent.

The complementarity problem formulation corresponding to the above conditions derived in Kwak and Lee (1988) is described for continuity. To describe the complementarity in the Coulomb friction law, an incremental relative slip value D_T at a contact point is expressed in terms of displacement increments and rigid body motion, and replaced with a difference of two non-negative variables as follows:

$$D_T \equiv D_T^+ - D_T^- = u_i^1 t_i^1 + u_i^2 t_i^2 - A_{ij} q_j, \tag{28}$$

$$D_T^+ \geqslant 0 \quad \text{and} \quad D_T^- \geqslant 0, \tag{29}$$

where t_i^1 and t_i^2 are tangential base vector components at the contact point as shown in Fig. 3, and A_{ij} represents the tangential displacement due to a unit displacement in the jth rigid body degree of freedom.

By introducing slack variables T^+ and T^-, eqn (27) can be rewritten as

$${}^{t+\Delta t}S_T + \mu^{t+\Delta t}P - T^+ = 0, \tag{30}$$

$${}^{t+\Delta t}S_T - \mu^{t+\Delta t}P + T^- = 0, \tag{31}$$

$$T^+ \geqslant 0 \quad \text{and} \quad T^- \geqslant 0. \tag{32}$$

The following complementarity conditions between slack variables are satisfied:

$$T^+ \cdot D_T^+ = 0, \tag{33}$$

$$T^- \cdot D_T^- = 0. \tag{34}$$

Similarly, eqn (19) can be rewritten in the following matrix form introducing slack variables V^+ and V^-:

$$\mathbf{A}_n^{Tt+\Delta t}\mathbf{P} + \mathbf{A}_t^{Tt+\Delta t}\mathbf{S}_T + \mathbf{H}^{Tt+\Delta t}\mathbf{F} + \mathbf{V}^- = 0, \tag{35}$$

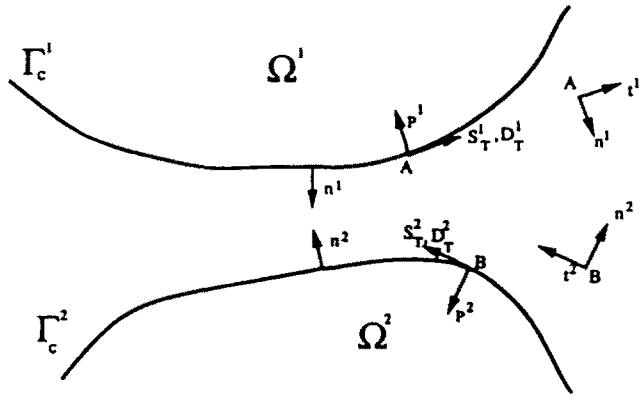

Fig. 3. Principal axes and force and relative displacement components at potential contact surface (Kwak, 1991).

$$\mathbf{A}_n^{T_t+\Delta t}\mathbf{P}+\mathbf{A}_t^{T_t+\Delta t}\mathbf{S}_T+\mathbf{H}^{T_t+\Delta t}\mathbf{F}-\mathbf{V}^+=0, \tag{36}$$

$$\mathbf{V}^+ \geqslant 0 \quad \text{and} \quad \mathbf{V}^- \geqslant 0. \tag{37}$$

Decomposing rigid body motion $\mathbf{q}$ with non-negative variables $\mathbf{q}^+$ and $\mathbf{q}^-$, the following complementarity conditions are also derived:

$$\mathbf{V}^+ \cdot \mathbf{q}^+ = 0, \tag{38}$$

$$\mathbf{V}^- \cdot \mathbf{q}^- = 0. \tag{39}$$

Using eqn (18) and summarizing eqns (25), (28), (30), (31), (35) and (36), a linear complementarity problem is derived as follows (Kwak, 1991):

$$\mathbf{z} = \mathbf{M}\mathbf{w}+\mathbf{r}, \tag{40}$$

$$\mathbf{w}^T\mathbf{z} = 0, \tag{41}$$

$$\mathbf{w} \geqslant 0 \quad \text{and} \quad \mathbf{z} \geqslant 0, \tag{42}$$

where

$$\mathbf{z} = \{\mathbf{D}_n \quad \mathbf{D}_T^+ \quad \mathbf{T}^- \quad \mathbf{V}^+ \quad \mathbf{V}^-\}^T,$$
$$\mathbf{w} = \{^{t+\Delta t}\mathbf{P} \quad \mathbf{T}^+ \quad \mathbf{D}_T^- \quad \mathbf{q}^+ \quad \mathbf{q}^-\}^T,$$

$$\mathbf{M} = \begin{bmatrix} \mathbf{B}_{nn}-\mathbf{B}_{nt}\mu & \mathbf{B}_{ni} & \mathbf{0} & -\mathbf{A}_n & \mathbf{A}_n \\ \mathbf{B}_{tn}-\mathbf{B}_{tt}\mu & \mathbf{B}_{ti} & \mathbf{I} & -\mathbf{A}_t & \mathbf{A}_t \\ 2\mu\mathbf{I} & -\mathbf{I} & \mathbf{0} & \mathbf{0} & \mathbf{0} \\ \mathbf{A}_n^T-\mathbf{A}_t^T\mu & \mathbf{A}_t^T & \mathbf{0} & \mathbf{0} & \mathbf{0} \\ -\mathbf{A}_n^T+\mathbf{A}_t^T\mu & -\mathbf{A}_t^T & \mathbf{0} & \mathbf{0} & \mathbf{0} \end{bmatrix}, \tag{43}$$

$$\mathbf{r} = \{\boldsymbol{\beta}+\mathbf{F}_n \quad \mathbf{F}_t \quad \mathbf{0} \quad \mathbf{H}^{T_t+\Delta t}\mathbf{F} \quad -\mathbf{H}^{T_t+\Delta t}\mathbf{F}\}^T. \tag{44}$$

3. SENSITIVITY ANALYSIS

The contact problem formulated above by eqns (40)–(42) can be transformed to an equivalent quadratic problem:

$$\text{Min } f_0 = \mathbf{w}^T(\mathbf{M}(\mathbf{b})\mathbf{w}+\mathbf{r}(\mathbf{b})), \tag{45}$$

$$\mathbf{z} = \mathbf{M}(\mathbf{b})\mathbf{w}+\mathbf{r}(\mathbf{b}) \geqslant 0, \tag{46}$$

$$\mathbf{w} \geqslant 0, \tag{47}$$

where a general parameter vector $\mathbf{b}$ is introduced to represent design parameters, loading scale factor or material properties.

The sensitivity analysis of interest concerns the effect of perturbations of the parameter on the optimal solution point. In this paper, the approximation scheme based on parametric optimal design (Kwak and Haug, 1976), is employed to obtain the sensitivity formula as

$$\delta\mathbf{w} = -\mathbf{D}\delta\mathbf{b}-\mathbf{C}, \tag{48}$$

where $\delta\mathbf{w}$ and $\delta\mathbf{b}$ are the variations of solution vector and problem parameter vector, respectively. Matrices $\mathbf{C}$ and $\mathbf{D}$ are given in the appendix for a general parametric optimal design.

In the above quadratic problem, the solution vector $\mathbf{w}$ is n-dimensional, but the number of constraints is $2n$. From the complementarity relationship between $\mathbf{z}$ and $\mathbf{w}$, n constraints are always active. If $\mathbf{w}$ is considered as basic variables ($\mathbf{w} > 0$) and $\mathbf{z}$ as non-basic variables ($\mathbf{z} = 0$) in complementarity pairs, only eqn (46) are active constraints. If constraints (46) are linearly independent, $\mathbf{M}_{qq}$ and $\Phi^{-1}\mathbf{M}_q$ in the appendix become a unit matrix and $\mathbf{M}(\mathbf{b})^{-1}$, respectively. This means that variations of solution variables are obtained by considering active constraints only, and matrices $\mathbf{C}$ and $\mathbf{D}$ are reduced to the simple form:

$$\mathbf{D} = \mathbf{M}(\mathbf{b})^{-1}\tilde{\mathbf{G}}^{\mathrm{T}}, \tag{49}$$

$$\mathbf{C} = -\mathbf{M}(\mathbf{b})^{-1}\Delta\tilde{\mathbf{g}}, \tag{50}$$

where $\Delta\tilde{\mathbf{g}}$ is the desired reduction in active constraints usually taken as $\Delta\tilde{\mathbf{g}} = -\tilde{\mathbf{g}}$ which corresponds to the amount of active constraint violation, and $\tilde{\mathbf{G}}^{\mathrm{T}}$ is given in the appendix. If problem parameters are fixed ($\delta\mathbf{b} = 0$), the solution is updated iteratively as

$$\mathbf{w}^{(k+1)} = \mathbf{w}^{(k)} + \mathbf{C}^{(k)}. \tag{51}$$

If the maximum violation constraint is considered for an iteration, this scheme is the same as the Lemke algorithm (Bazaraa and Shetty, 1979) for linear complementarity problems. At a solution point, $\mathbf{C}$ equal to zero since constraint villations $\Delta\tilde{\mathbf{g}}$ are zero. Then the variation of a solution point with respect to a problem parameter perturbation $\delta\mathbf{b}$ is given as

$$\delta\mathbf{w} = -\mathbf{D}\delta\mathbf{b}. \tag{52}$$

From the solution scheme, the sensitivity matrix $\mathbf{D}$ is obtained if $\tilde{\mathbf{G}}^{\mathrm{T}}$ is used as another loading vector since $\mathbf{w}$ is a basic solution vector. At a solution point, there is a small range of parameter perturbations such that the set of active constraints is not changed for small perturbations of problem parameters. So the variation of the non-basic solution $\mathbf{z}$ is zero.

For a degenerate case, that is, when both $z_i = 0$ and $w_i = 0$ for an i, the number of active constraints can be greater than n. In this case, different sensitivity matrices $\mathbf{D}$ are obtained by choosing different sets of n active constraints from the active constraint set. Each of these different sensitivity matrices $\mathbf{D}$ denotes a directional derivative at the solution point for the degenerate case. Sensitivity results are used for the determination of a suitable load increment as described below.

4. NUMERICAL IMPLEMENTATION AND EXAMPLES

Since the solution of a contact problem is loading-path dependent, a load increment is calculated by considering the contact status at loading step t. According to the sensitivity results, the variations of the basic solution $\mathbf{w}$ and non-basic solution $\mathbf{z}$ at loading step t for a loading perturbation δf are obtained as

$$\delta\mathbf{w} = -\mathbf{D}\delta f, \tag{53}$$

$$\delta\mathbf{z} = 0, \tag{54}$$

where the sensitivity matrix $\mathbf{D}$ is

$$\mathbf{D} = -\mathbf{M}^{-1}\mathbf{G}^{\mathrm{T}}, \tag{55}$$

$$\mathbf{G}^{\mathrm{T}} = \{\delta\mathbf{F}_n \quad \delta\mathbf{F}_t \quad \mathbf{0} \quad -\mathbf{H}^{\mathrm{T}}\delta^{t+\Delta t}\mathbf{F} \quad \mathbf{H}^{\mathrm{T}}\delta^{t+\Delta t}\mathbf{F}\}^{\mathrm{T}}. \tag{56}$$

Here $\mathbf{M}$ is the same matrix as in eqn (43) for the basic solution $\mathbf{w}$ and non-basic solution $\mathbf{z}$ at loading step t, and $\mathbf{G}^{\mathrm{T}}$ is the variation of the force vector $\mathbf{r}$ in eqn (44).

After load increment Δf, basic solutions ${}^{t+\Delta t}\mathbf{w}$ at loading step $t+\Delta t$ are expected to be

$$ {}^{t+\Delta t}\mathbf{w} = {}^{t}\mathbf{w} - \mathbf{D}\Delta f. \tag{57} $$

For a change in the contact status, at least one component of the basic solution ${}^{t+\Delta t}\mathbf{w}$ will be reduced to zero at loading step $t+\Delta t$. So the load increment Δf is calculated with the following provisions:

(i) load increment for a contact point to be a non-contact point

If the contact normal force ${}^{t}P_i$ for a contact point i is a basic solution at loading step t, ${}^{t+\Delta t}P_i$ at loading step $t+\Delta t$ is expected to be

$$ {}^{t+\Delta t}P_i = {}^{t}P_i + \frac{\partial P_i}{\partial f}\Delta f, \tag{58} $$

where $P_i' \equiv (\partial P_i/\partial f)$ can be obtained from (53) by considering a unit variation of δf. Then the load increment Δf_{P_i} that can make ${}^{t+\Delta t}P_i$ be zero is

$$ \Delta f_{P_i} = -\frac{{}^{t}P_i}{P_i'}. \tag{59} $$

(ii) load increment for a non-contact point to be a contact point

If the contact gap ${}^{t}D_{n_i}$ for a contact point i is a basic solution at loading step t, ${}^{t+\Delta t}D_{n_i}$ at loading step $t+\Delta t$ is expected to be

$$ {}^{t+\Delta t}D_{n_i} = {}^{t}D_{n_i} + \frac{\partial D_{n_i}}{\partial f}\Delta f. \tag{60} $$

As in the previous case, to reduce ${}^{t+\Delta t}D_{n_i}$ to zero, the load increment Δf_{D_i} is

$$ \Delta f_{D_i} = -\frac{{}^{t}D_{n_i}}{D_{n_i}'}, \tag{61} $$

where $D_{n_i}' \equiv (\partial D_{n_i}/\partial f)$ can be obtained from (53) by considering a unit variation of δf.

(iii) load increment for a stick contact point to be a slip contact point

If slack variables T_i^+ and T_i^- for a contact point i are basic solutions at loading step t, the tangential contact force ${}^{t+\Delta t}S_{T_i}$ at loading step $t+\Delta t$ is expected to be

$$ \begin{aligned} {}^{t+\Delta t}S_{T_i} &= {}^{t}S_{T_i} + \frac{\partial S_{T_i}}{\partial f}\Delta f \\ &= ({}^{t}T_i^+ - {}^{t}T_i^-)/2 + \left(\frac{\partial T_i^+}{\partial f} - \frac{\partial T_i^-}{\partial f}\right)\Delta f/2, \end{aligned} \tag{62} $$

where $S_{T_i}' \equiv (\partial S_{T_i}/\partial f)$ can be obtained from (53) by considering a unit variation of δf. If slip is to occur at $t+\Delta t$, the tangential contact force ${}^{t+\Delta t}S_{T_i}$ must be

$$ {}^{t+\Delta t}S_{T_i} = \pm(\mu\,{}^{t+\Delta t}P_i). \tag{63} $$

Inserting eqns (58) and (62) into (63), the load increment for slip to occur is determined as

$$ \Delta f_{s^+} = \frac{\mu\,{}^{t}P_i - {}^{t}S_{T_i}}{S_{T_i}' - \mu P_i'} \tag{64} $$

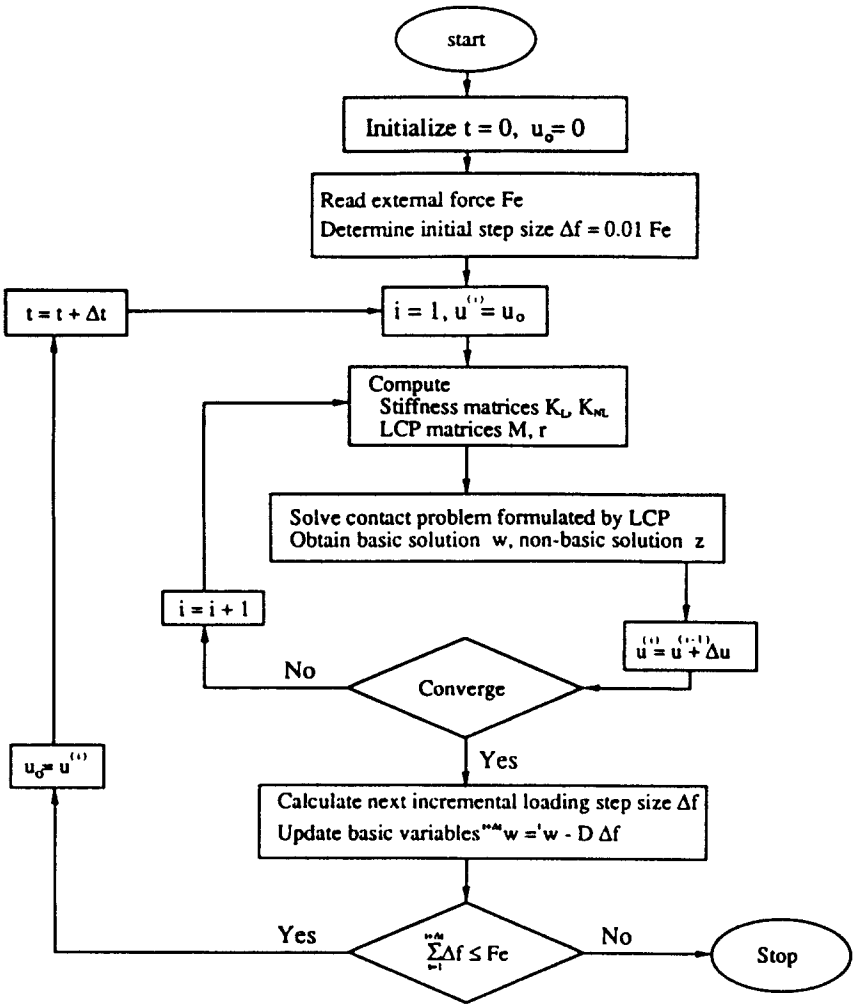

Fig. 4. Block diagram of the present computer algorithm for contact stress analysis with Coulomb friction.

or

$$\Delta f_s = -\frac{(\mu {}^{t}P_i + {}^{t}S_i)}{S'_i + \mu P'_i}. \tag{65}$$

The smallest load increment is selected to follow the load history:

$$\Delta f = \min = \{\Delta f_{P_i}, \Delta f_{D_i}, \Delta f_{s'}, \Delta f_s\}. \tag{66}$$

Now, an initial basic variable $^{t+\Delta t}w$ can be obtained from eqn (57). And the solution point at $t+\Delta t$ is obtained iteratively from eqn (51). The proposed solution scheme for a contact problem with friction is thus summarized as shown in Fig. 4. It is noted that the step-size problem with non-constant coefficient matrices for elasto-plastic large deformation is yet to be studied.

Example 1. Frictional slip between a layer and half-plane due to a periodic tangential force

In this example, the contact phenomena between an elastic layer and a half-plane due to concentrated surface loads have been examined and compared with the solutions by Comninou and Barber (1983). The layer of thickness a is pressed against the half-plane by a uniform pressure P_0 as shown in Fig. 5, and subjected to a concentrated tangential load

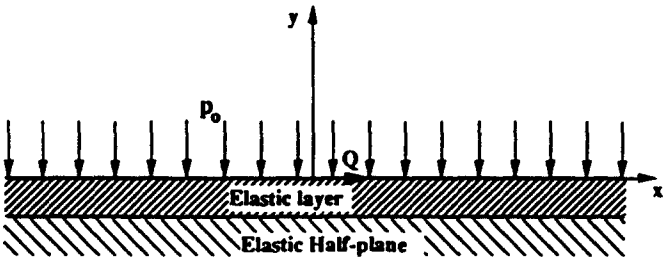

Fig. 5. Layer–substrate geometry.

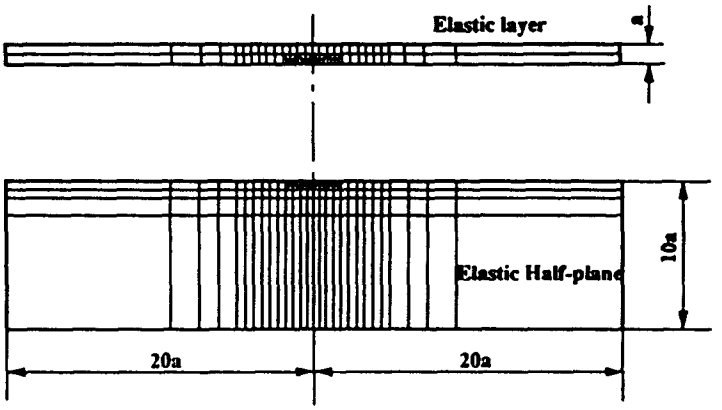

Fig. 6. FEM model of a layer and a half-plane.

Q which varies periodically in time as shown in Fig. 7. For the layer and the half-plane, 72 quadrilateral plane strain finite elements and 128 elements are used respectively as shown in Fig. 6, and 39 contact nodes are used in the potential contact surface between the layer and the half-plane. Young's modulus, Poisson's ratio and Coulomb's frictional coefficient are 200,000 (force/length^2), 0.3 and 0.5, respectively. In the description of results, dimensionless loading parameter $\lambda = (Q/P_0a)$ (and corresponding $\lambda_1 = (Q_1/P_0a)$) is used as in

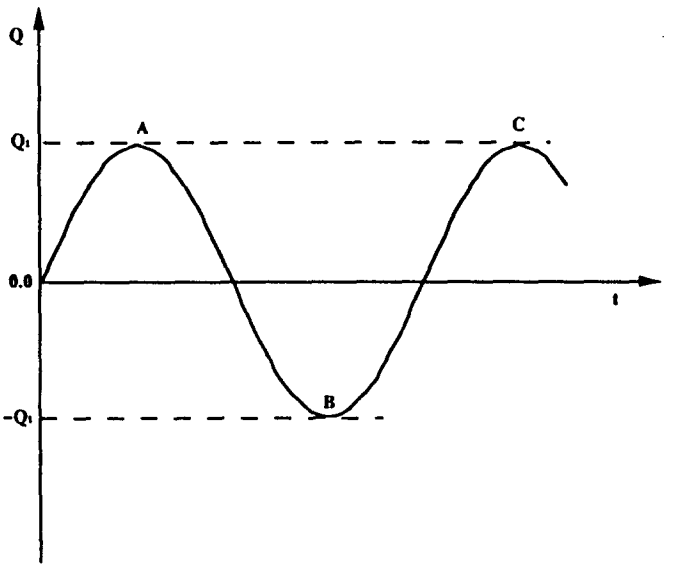

Fig. 7. Variation of load Q as a function of time.

Comninou and Barber (1983). In this numerical computation, λ_1 is taken as 2.353 and friction coefficient μ as 0.5 for comparison with the existing solution.

Initially a uniform pressure P_0 is applied and $\lambda = 0.01\ \lambda_1$ is taken as the first load increment. The loading when the first slip occurs is calculated from the sensitivity results. The first slip occurs when $\lambda = 2.054$, and slip region increases to $-1.5 < x\ a < -0.5$ when $\lambda = \lambda_1$. During unloading, stick prevails everywhere until $\lambda = -2.057$, and then back slip occurs in the range $0.5 < x/a < 1.5$ when $\lambda = -\lambda_1$. According to Comninou and Barber (1983), the first slip occurs when $\lambda = 2.03$, forward slip occurs in the range $-1.4445 < x/a < -0.4$ during the first loading and back slip occurs in $0.4039 < x/a < 1.4391$ during unloading. In the present numerical calculation, the forward slip area on loading and the back slip area on unloading are the same possibly because of the size of the discretization. But it is found that back slip occurs at a higher load than the first forward slip by the effect of the residual frictional force. During reloading to λ_1, no slip occurs anywhere. In the calculation process, four loading steps on loading, four on unloading and two on reloading have been executed as determined by the sensitivity results. The normal contact pressure and shear traction distributions are shown in Figs 8 and 9 and compared with the solutions redrawn manually from Comninou and Barber (1983). By an increase of the maximum tangential force Q_1, the slip region extends and slip occurs on reloading when $\lambda_1 = 3.051$ [$\lambda_1 = 3.1$ by Comninou and Barber (1983)]. The overall behavior of the slip–nonslip history, the corresponding loads levels and traction distributions are all in good agreement with the analytical solution from Comninou and Barber (1983).

Example 2. Three body frictional contact analysis of a valve-cotter system of a motorcycle engine

The intake valve shown in Fig. 10 taken from a motorcycle engine is driven by cam and locker arm. At the initial position with the valve closed, the two springs are in a compressed state pressing the cotter and the retainer. By the motion of the valve, the spring

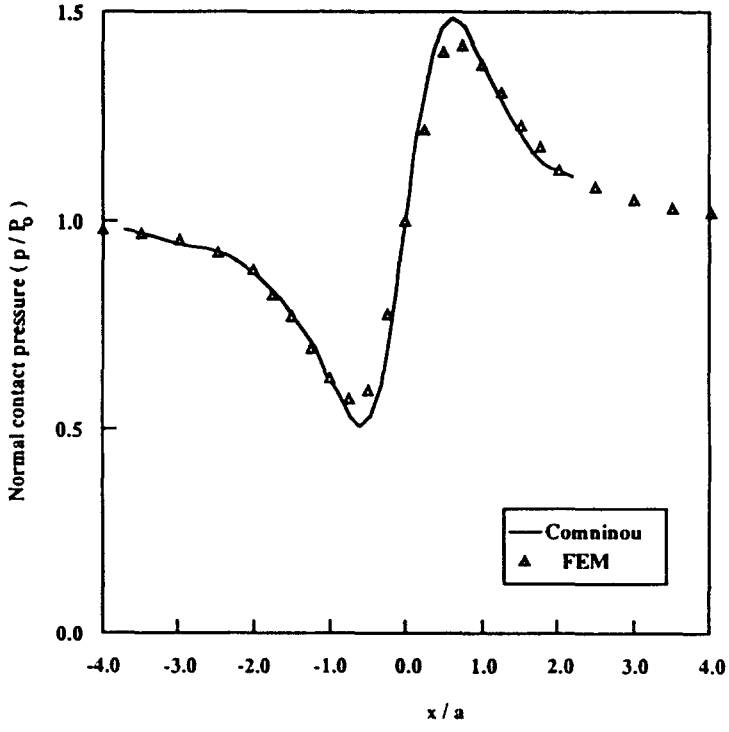

Fig. 8. Normal contact pressure for $\lambda_1 = 2.353$. (a) Loading corresponding to point A in Fig. 7. (b) Loading corresponding to point B in Fig. 7. (c) Loading corresponding to point C in Fig. 7.

(b)

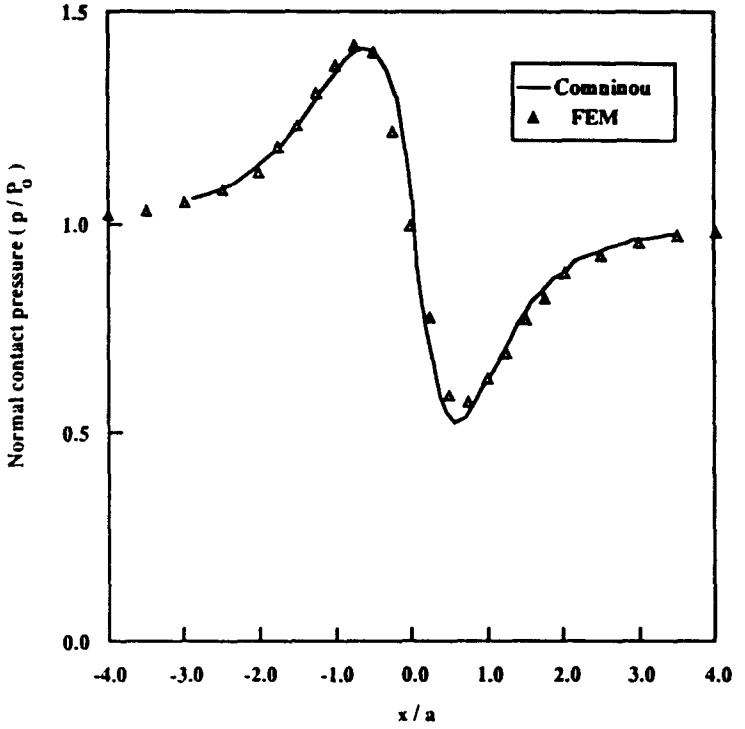

(c)

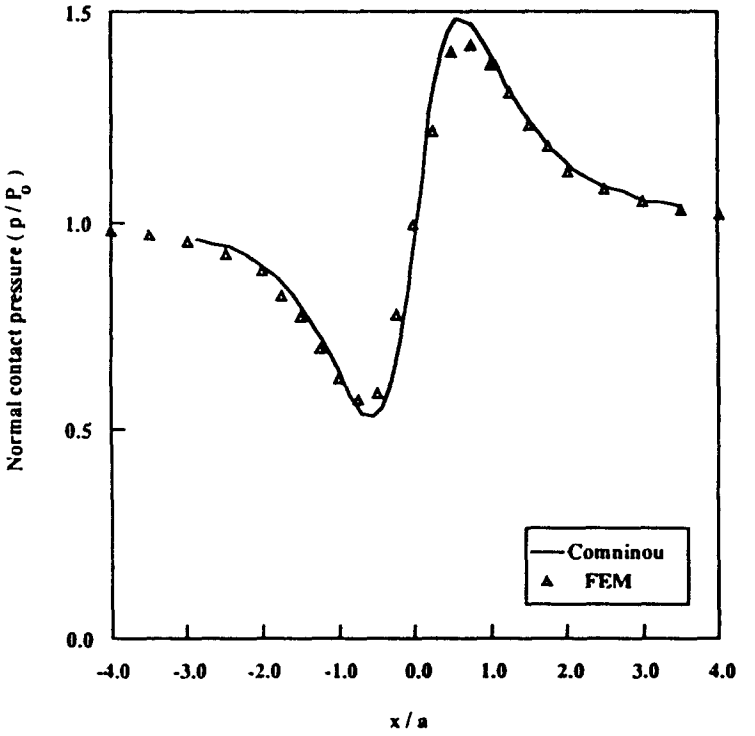

Fig. 8 *continued*

forces oscillate. The extent of contact pressure concentration and the prediction of wear due to the frictional slip during this repeated loading will be the most important information for the design of the system.

The valve-cotter system is analysed as a three body frictional contact problem. The valve, the cotter and the retainer are modeled by 105, 133 and 86 quadrilateral axisymmetric

finite elements respectively as shown in Fig. 11. Young's modulus, Poisson's ratio and the friction coefficient are taken as 206 GPa, 0.3 and 0.3, respectively. In this model, the vertical displacement of point a in Fig. 11 is fixed. The cotter and the retainer are allowed to have rigid body motions in the z direction. The spring forces varying periodically in time as

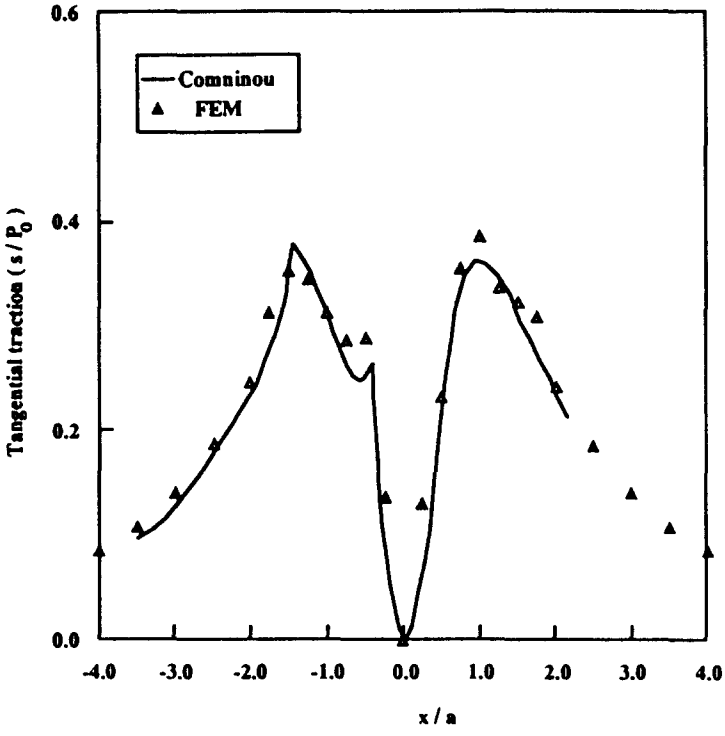

(a)

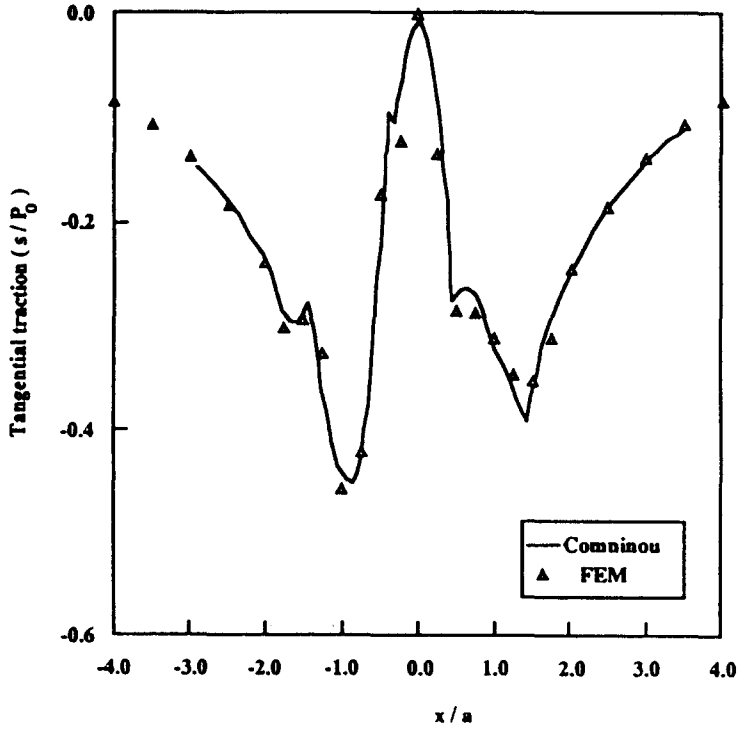

(b)

Fig. 9. Tangential traction for $\lambda_1 = 2.353$. (a) Loading corresponding to point A in Fig. 7. (b) Loading corresponding to point B in Fig. 7. (c) Loading corresponding to point C in Fig. 7.

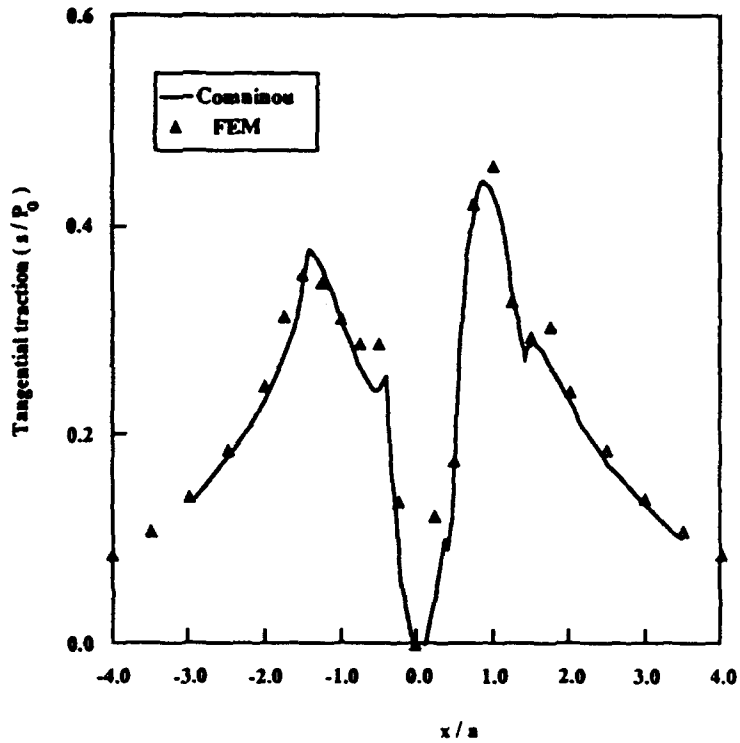

(c)

Fig. 9 *continued*

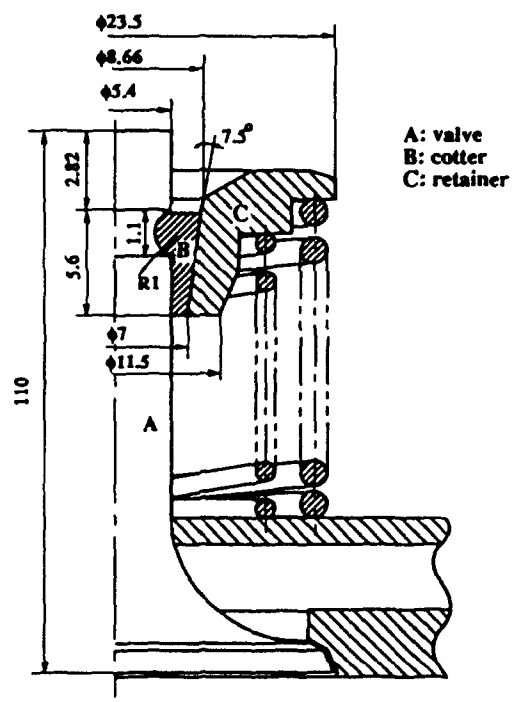

Fig. 10. Valve-cotter system of a motorcycle engine (Courtesy of Hyosung Machineries, Inc.).

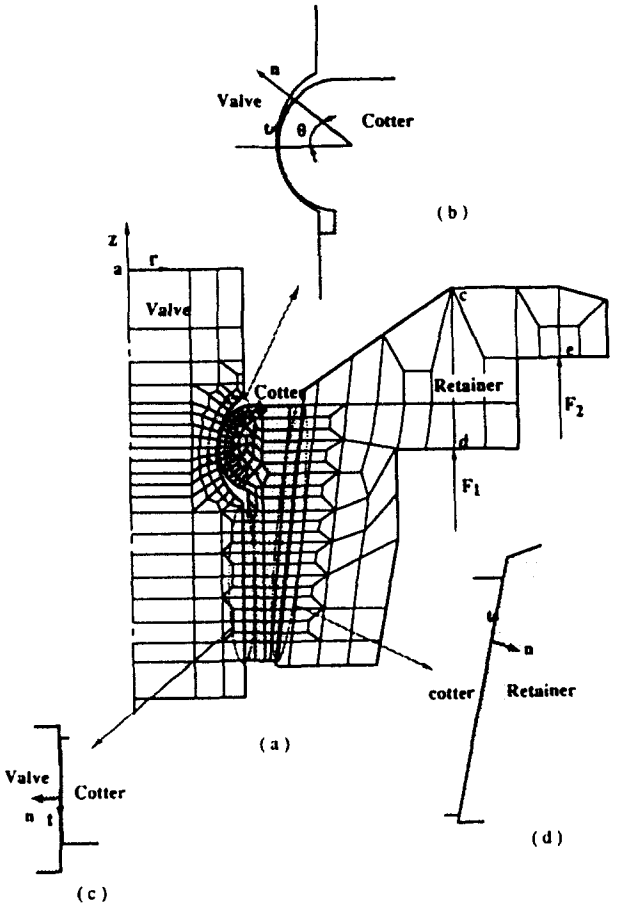

Fig. 11. FEM model of valve, cotter and retainer and coordinates of contact region. (a) FEM model. (b) Contact region 1. (c) Contact region 2. (d) Contact region 3.

shown in Fig. 12 are acting at points d and e in Fig. 11. They are estimated from a separated analysis of the valve system. Three potential contact regions are identified: Regions 1 and

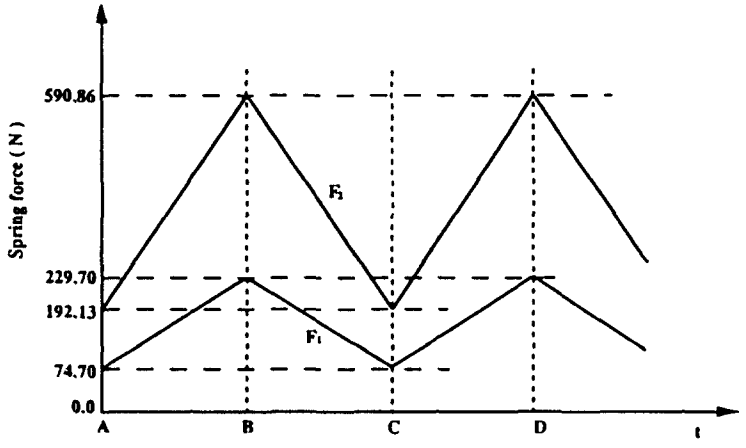

Fig. 12. Spring forces as a function of time.

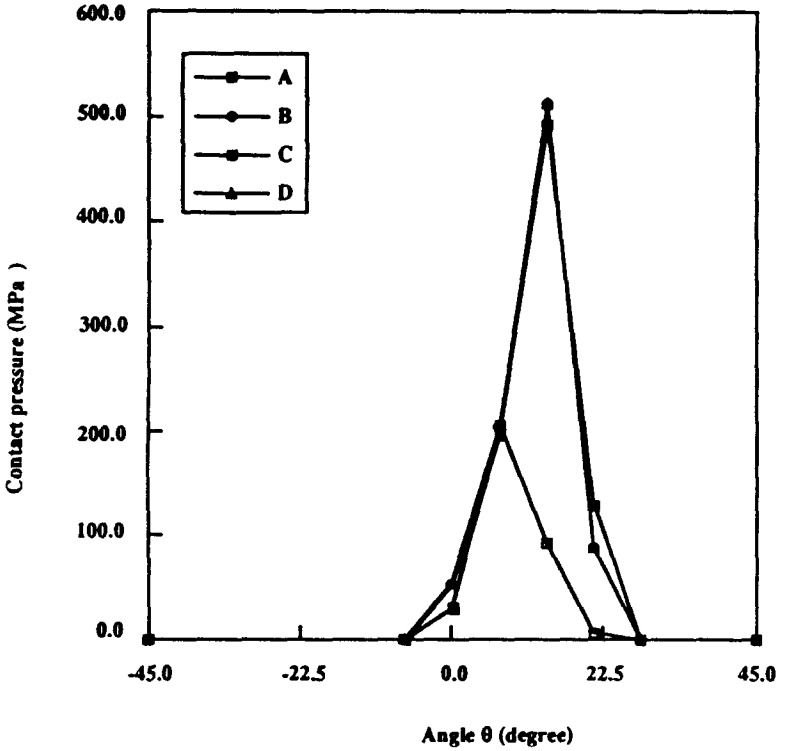

Fig. 13. Pressure distributions in potential contact region I for various load levels in Fig. 12.

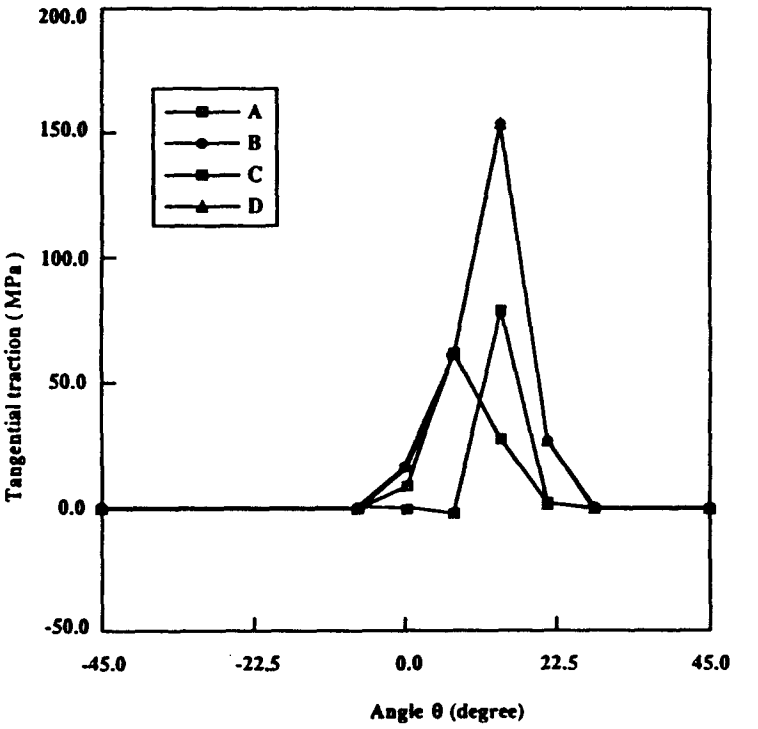

Fig. 14. Tangential traction distributions in potential contact region I for various load levels in Fig. 12.

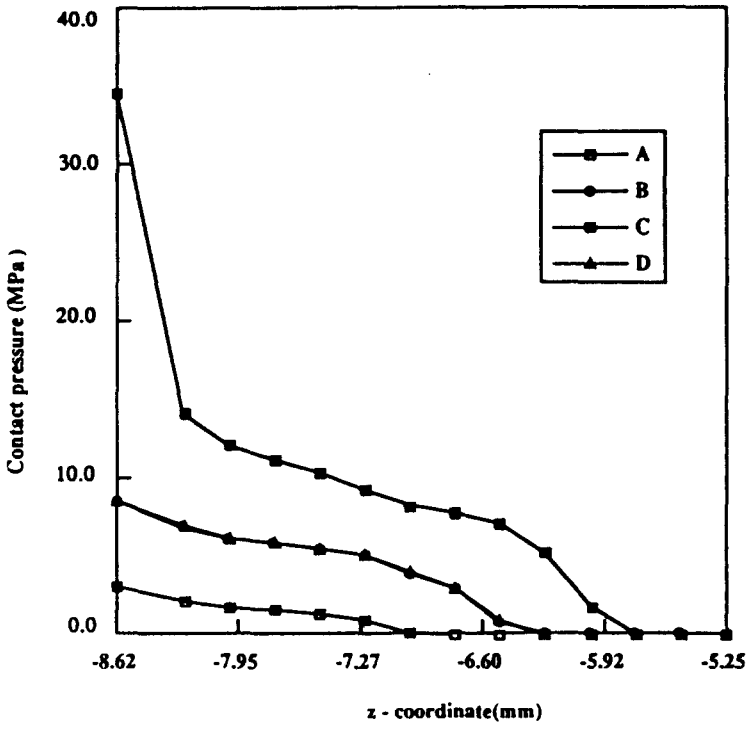

Fig. 15. Pressure distributions in potential contact region 2 for various load levels in Fig. 12.

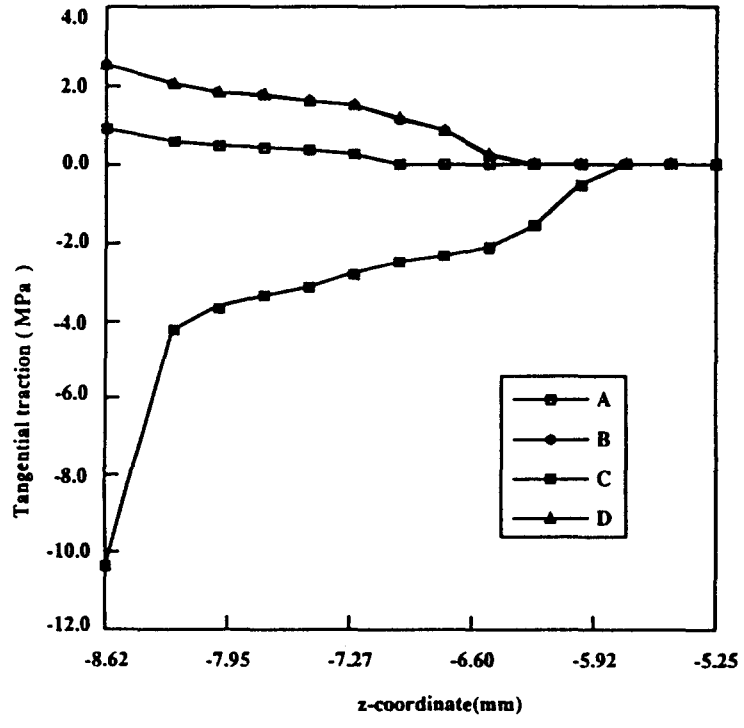

Fig. 16. Tangential traction distributions in potential contact region 2 for various load levels in Fig. 12.

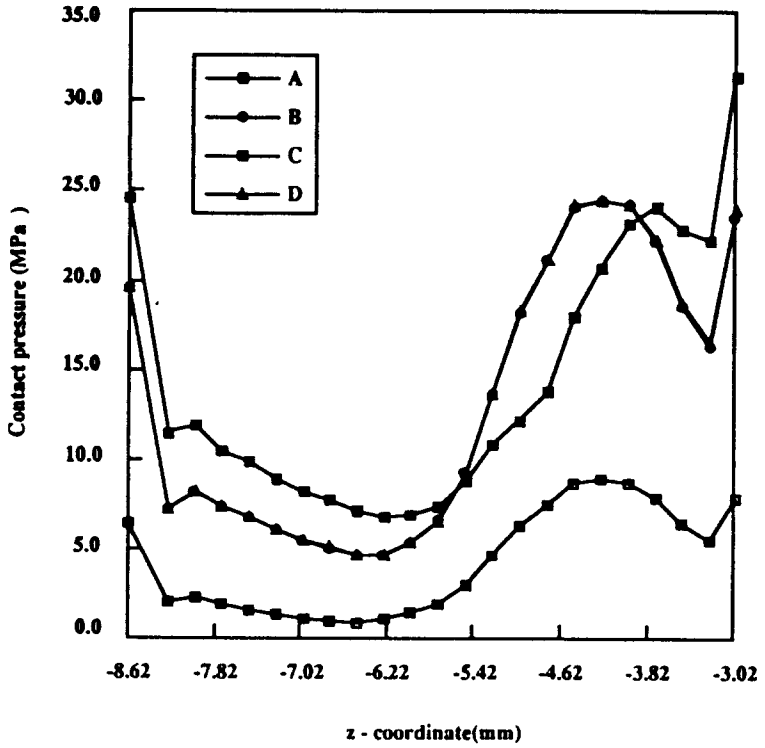

Fig. 17. Pressure distributions in potential contact region 3 for various load levels in Fig. 12.

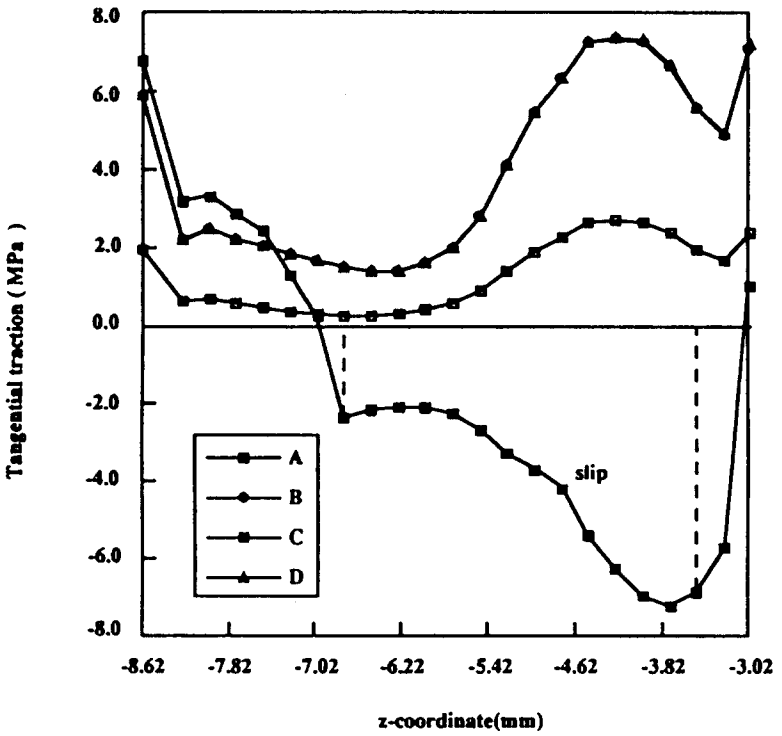

Fig. 18. Tangential traction distributions in potential contact region 3 for various load levels in Fig. 12.

2 between the valve and the cotter with 10 and 14 nodes, respectively, and region 3 between the cotter and the retainer with 23 nodes, as shown in Fig. 11(b), (c) and (d).

During the first loading between time A and B in Fig. 12, all of the nodes in contact region 1 are in a state of slip and the contact pressure is highest in this region as shown in Fig. 13. In the unloading stage between B and C, back slip occurs at all nodes in contact region 2. But, in contact region 3, back slip occurs in the middle zone as shown in Fig. 18 and the other nodes near both ends are in a state of stick. No slip occurs in contact region 1. The contact pressure and tangential traction show very much different distributions for the same load levels A and C. The distributions at time B on loading and at D on reloading, however, are nearly equal indicating that the contact status is repeating after time B.

As noted by Torstenfelt (1984), stress at a point is not necessarily at its extreme when the external load becomes maximum. For all of the contact nodes in region 2 and the nodes at end zone in region 3, the normal contact pressure and the tangential traction are larger at time C than at B and D although external load at C is smallest. This is due to the frictional effect as shown in Figs 15–18. The contact pressure concentration at region 1 and slip and back slip at region 2 and 3 can be damaging to the cotter. Because of the rapid change of the contact status, 6 loading steps on loading, 15 on unloading and 24 on reloading have been found performed in the incremental analysis.

5. CONCLUSION

A sensitivity analysis for the frictional contact formulated by complementarity is presented and used for a logical determination of load increments. The algorithm developed is very efficient and systematic. The method has been applied to the case of a periodic tangential loading of an elastic layer and a half-plane. The results agree well with the analytical solutions by Comninou and Barber. As a practical application, a valve-cotter system of a motorcycle engine has been solved as a three body frictional contact problem. The results have shown the capability of following a complex response history and revealed all the detail information necessary for a design analysis.

Acknowledgement—The authors acknowledge the support of Korea Science and Engineering Foundation.

REFERENCES

Bathe, K. J. (1982). *Finite Element Procedures in Engineering Analysis*. Prentice-Hall, New Jersey.

Bazaraa, M. and Shetty, C. M. (1979). *Nonlinear Programming Theory and Algorithms*. Wiley, New York.

Bendsoe, M. P., Olhoff, N. and Sokolowski, J. (1985). Sensitivity analysis of problems of elasticity with unilateral constraints. *J. Struct. Mech.* **13**, 201–222.

Comninou, M. and Barber, J. R. (1983). Frictional slip between a layer and a substrate due to a periodic tangential surface force. *Int. J. Solids Structures* **19**, 533–539.

Duvaut, G. and Lions, J. L. (1976). *Inequalities in Mechanics and Physics*. Springer, New York.

Fiacco, A. V. and Ghaemi, A. (1982). Sensitivity analysis of a nonlinear structural design problem. *Comput. Ops. Res.* **9**, 29–55.

Hanson, M. T. and Keer, L. M. (1989). Cyclic tangential loading of dissimilar elastic bodies. *Int. J. Mech. Sci.* **31**, 107–119.

Haslinger, J. and Heittaanmaki, P. (1988). *Finite Element Approximation for Optimal Shape Design: Theory and Application*. Wiley, New York.

Jittorntrum, K. (1984). Solution point differentiability without strict complementarity in nonlinear programming. *Math. Program.* **21**, 127–138.

Joo, J. W. and Kwak, B. M. (1986). Analysis and applications of elasto-plastic contact problems considering large deformation. *Comput. Struct.* **24**, 953–961.

Klarbring, A. (1986). General contact boundary conditions and the analysis of frictional systems. *Int. J. Solids Structures* **22**, 1377–1398.

Kwak, B. M. (1990). Numerical implementation of three-dimensional frictional contact by a linear complementarity problem. *KSME Jl* **4**, 23–31.

Kwak, B. M. (1991). Complementarity problem formulation of three-dimensional frictional contact. *ASME J. Appl. Mech.* **113**, 134–140.

Kwak, B. M. and Haug, E. J. (1976). Parametric optimal design. *J. Opt. Theory and Appl.* **20**, 13–35.
Kwak, B. M. and Lee, S. S. (1988). A complementarity problem formulation for two-dimensional frictional contact problems. *Comput. Struct.* **28**, 469–480.
Oden, J. T. and Pires, E. B. (1983a). Nonlocal and nonlinear friction laws and variational principles for contact problems in elasticity. *ASME J. Appl. Mech.* **50**, 67–76.
Oden, J. T. and Pires, E. B. (1983b). Analysis of contact problems with friction under oscillating loads. *Comp. Meth. Appl. Mech. Engng* **39**, 337–362.
Okamoto, N. and Nakazawa, M. (1979). Finite element incremental contact analysis with various frictional conditions. *Int. J. Numer. Meth. Engng* **14**, 337–357.
Panagiotopoulos, P. D. (1985). *Inequality Problems in Mechanics and Applications*. Birkhaeuser, Boston.
Rahman, M. U., Rowlands, R. E. and Cook, R. D. (1984). An iterative procedure for finite element stress analysis of frictional contact problems. *Comput. Struct.* **18**, 947–954.
Tobin, R. L. (1986). Sensitivity analysis for variational inequalities. *J. Opt. Theory and Appl.* **48**, 191–204.
Torstenfelt, B. (1984). An automatic incrementation technique for contact problems with friction. *Comput. Struct.* **19**, 393–400.
Sokolowski, J. (1988). Sensitivity analysis of contact problems with prescribed friction. *Appl. Math. Optim.* **18**, 99–117.

APPENDIX: FIRST-ORDER SENSITIVITY FORMULA FOR AN OPTIMAL PROBLEM

An explicit expression for the first-order sensitivity formula by Kwak and Haug (1976) is shown using a gradient-projection method with constraint error compensation. The problem is of the following type:

$$\min_{\mathbf{w}} f_0(\mathbf{w}, \mathbf{b}), \tag{A1}$$

$$\text{subject to } \mathbf{g}(\mathbf{w}, \mathbf{b}) \leqslant 0, \tag{A2}$$

where $\mathbf{b}$ is the vector of problem parameters and $\mathbf{w}$ solution vector.

An approximation problem is defined by Taylor series expansions of the objective function f_0 up to the second order and active constraints up to the first order as follows:

$$\min_{\delta \mathbf{w}} \delta f_0 \equiv \left(\frac{\partial f_0}{\partial \mathbf{b}}\right)\delta \mathbf{b} + \left(\frac{\partial f_0}{\partial \mathbf{w}}\right)\delta \mathbf{w} + \frac{1}{2}\delta \mathbf{b}^{\mathrm{T}}\left(\frac{\partial^2 f_0}{\partial \mathbf{b}^2}\right)\delta \mathbf{b} + \delta \mathbf{b}^{\mathrm{T}}\left(\frac{\partial^2 f_0}{\partial \mathbf{b}\,\partial \mathbf{w}}\right)\delta \mathbf{w} + \frac{1}{2}\delta \mathbf{w}^{\mathrm{T}}\left(\frac{\partial^2 f_0}{\partial \mathbf{w}^2}\right)\delta \mathbf{w}, \tag{A3}$$

$$\delta \tilde{\mathbf{g}} \equiv \frac{\partial \tilde{\mathbf{g}}}{\partial \mathbf{w}}\delta \mathbf{w} + \frac{\partial \tilde{\mathbf{g}}}{\partial \mathbf{b}}\delta \mathbf{b} = \Delta \tilde{\mathbf{g}}, \tag{A4}$$

where $\Delta \tilde{\mathbf{g}}$ is the desired reduction in the active constraints.

The Kuhn–Tucker necessary conditions for the problem (A3)–(A4) are then solved to obtain

$$\delta \mathbf{w} = -\mathbf{D}\delta \mathbf{b} - \mathbf{C}, \tag{A5}$$

where

$$\mathbf{D} = \Phi^{-1}[(\mathbf{I} - \mathbf{M}_{yy})\mathbf{B}^{\mathrm{T}} + \mathbf{M}_y \tilde{\mathbf{G}}^{\mathrm{T}}],$$

$$\mathbf{C} = \Phi^{-1}[(\mathbf{I} - \mathbf{M}_{yy})\mathbf{A} - \mathbf{M}_y \Delta \tilde{\mathbf{g}}],$$

$$\mathbf{M}_y = \tilde{\mathbf{Q}}(\tilde{\mathbf{Q}}^{\mathrm{T}}\Phi^{-1}\tilde{\mathbf{Q}})^{-1}, \quad \mathbf{M}_{yy} = \mathbf{M}_y \tilde{\mathbf{Q}}^{\mathrm{T}}\Phi^{-1},$$

$$\Phi = \frac{\partial^2 f_0}{\partial \mathbf{w}^2}, \quad \tilde{\mathbf{Q}}^{\mathrm{T}} = \frac{\partial \tilde{\mathbf{g}}}{\partial \mathbf{w}}, \quad \tilde{\mathbf{G}}^{\mathrm{T}} = \frac{\partial \tilde{\mathbf{g}}}{\partial \mathbf{b}}, \quad \mathbf{B}^{\mathrm{T}} = \frac{\partial^2 f_0}{\partial \mathbf{b}\,\partial \mathbf{w}}, \quad \mathbf{A} = \frac{\partial f_0}{\partial \mathbf{w}}.$$